Available online at www.sciencedirect.com
ScienceDirect
Polymer 49 (2008) 1199–1210
polymer
www.elsevier.com/locate/polymer

Synthesis of hybrid linear-dendritic block copolymers with carboxylic functional groups for the biomimetic mineralization of calcium carbonate

Lili Wang, Zhangle Meng, Yuelong Yu, Qingwei Meng, Dongzhong Chen*

Key Laboratory of Mesoscopic Chemistry of Ministry of Education and Department of Polymer Science and Engineering, School of Chemistry and Chemical Engineering, Nanjing University, 22 Hankou Road, Nanjing, Jiangsu 210093, PR China

Received 26 July 2007; received in revised form 3 January 2008; accepted 14 January 2008
Available online 18 January 2008

Abstract

A series of carboxylic acid functionalized hybrid linear-dendritic block copolymers (LDBCs) derived from methoxy poly(ethylene glycol) (MPEG) and variant generation dendrons from 2,2-bis(hydroxymethyl) propionic acid were synthesized and employed as $CaCO_3$ crystallization growth modifiers. Mainly spherical vaterite particles of gradually reduced sizes were produced with the increase of the polymer additive concentration and/or the dendron segment generation number, while the incorporated polymer organic components in the particles increased for the promoted binding efficiency and ever enhanced adsorption ability. A higher mineralization temperature resulted in significantly larger particle size and partly calcite formation. Under the same molar concentration of carboxylic acid, the same size level particles were obtained which manifested the crucial role of the functional group, meanwhile, the slight decrease of the spherical vaterite diameters with increasing generation number and especially the formation of particular pine-cone shaped calcite crystals also revealed the significant effect of the architectural structure of variant generations and some special characters of the hybrid LDBC structures.
© 2008 Elsevier Ltd. All rights reserved.

Keywords: Carboxylated linear-dendritic block copolymer; Crystallization modifier; Calcium carbonate

1. Introduction

Biominerals have unique structures and morphologies, which usually exhibit good mechanical strength with excellent toughness compared with the relatively crude minerals [1–3]. Calcium carbonate is the most common one among the over sixty kinds of biological minerals [4]. $CaCO_3$ has three anhydrous crystalline polymorphs, i.e., vaterite, aragonite, and calcite in order of increasing stability. Biomimetic synthesis of $CaCO_3$ under the influence of organic templates and/or additives has aroused intensive investigations in recent years as reviewed recently [5–9]. Langmuir monolayers and self-assembled films [10–15], foam lamellae [16,17], designed emulsion systems [18,19], and functionalized hydrogels [20,21], have been used as effective templates or additives for the controlled growth of $CaCO_3$ crystals, mainly on the control of polymorph, morphology and/or crystal orientation. Especially a kind of polymer additives so called double hydrophilic block copolymers (DHBCs) have been successfully employed in the biomimetic syntheses of inorganic minerals, which exert remarkably effective control over the size, shape, morphology and structure of $CaCO_3$ due to its separation of the binding and solving functions [22–31]. Recently a unifying model of polymer-mediated crystallization has been proposed based on the aggregation of precursor subunits [31]. Most of the DHBCs investigated so far are linear copolymers although some with branched or hyperbranched functional segments.

On the other hand, many research results have shown that selectivity for certain crystal faces appears to be highly dependent on the secondary structure of the macromolecule additives [32–34]. Dendrimers are a kind of synthetic polymers

* Corresponding author. Tel.: +86 25 83686621; fax: +86 25 83317761.
E-mail address: cdz@nju.edu.cn (D. Chen).

0032-3861/$ - see front matter © 2008 Elsevier Ltd. All rights reserved.
doi:10.1016/j.polymer.2008.01.023

possessing some features of biomacromolecules, for example, they have exact molecular weight, unique and well-defined secondary structures, in the early generations the starburst structures are of disklike shape, and the structures are of sphere in the higher generations [35]. Recently, poly(amidoamine) (PAMAM) dendrimers with carboxylic acid groups have been found to exert effective control on the $CaCO_3$ crystallization and result in the formation of stable spherical vaterite polymorph [36–38]. Furthermore, poly(propyleneimine) (PPI) dendrimers modified with long alkyl chains were reported to form remarkably rigid and well-defined aggregates, which templated the formation of interesting inorganic–organic hybrid materials [39,40]. Our recent research results showed that even the less regular hyperbranched aliphatic polyesters with carboxylic or sulfonic acid functional groups exhibited remarkable polymorph selectivity and morphology control. Under certain conditions well-defined core–shell structured vaterite spheres were obtained with obvious radial organization by nano-aggregation mechanism [41]. For their precise molecular structure, globular shape and high functionality of the dendrimer segment and the combination of variant linear and dendritic segments, hybrid linear-dendritic block copolymers (LDBCs) have been exploited for possible applications in variant fields as in surface modification [42], gene therapy [43,44], drug delivery [45,46] and stimuli-responsive devices [47,48]. Here we present the synthesis of a series of LDBCs derived from methoxy poly(ethylene glycol) (MPEG) and variant generation dendrons from 2,2-bis(hydroxymethyl) propionic acid (BMPA) according to a facile divergent strategy and then the hydroxyl groups were converted into carboxylic acid functional groups through reaction with succinic anhydride. The series carboxylated LDBCs were employed as $CaCO_3$ crystallization growth modifiers which exhibited very strong control ability both for crystal polymorphism and morphology. To the best of our knowledge, this is the first report of LDBCs as a modifier for the biomimetic mineralization.

2. Experimental

2.1. Materials

2,2-Bis(hydroxymethyl) propionic acid (BMPA), *p*-toluenesulfonic acid (*p*-TSA), succinic anhydride (SA), *N*,*N*′-dicyclohexylcarbodiimide (DCC), 4-(dimethylamino) pyridine (DMAP) and methoxy poly(ethylene glycol) (MPEG) (M_n ca. 5000 g/mol) were purchased from Aldrich. All other chemicals were of analytical grade and used without further purification and all solvents were distilled prior to use.

2.2. Characterization

^{1}H NMR spectra were recorded on a 300 MHz (Bruker AMX300) spectrometer with the residual proton signals of solvents as internal standards. Gel-permeation chromatography (GPC) was performed on Waters 244 with differential refractometer R401 fitted with four ultrastyragel columns having pore sizes 100, 500, 10^3, 10^4 Å. THF was used as eluent at a flow rate of 1 mL/min and the molecular weight calculation was based on linear polystyrene standards. Fourier transform infrared spectra (FTIR) were recorded on a NICOLET TNEXUS870 infrared spectrometer with pressed potassium bromide pellets. Scanning electron microscopy (SEM) images were obtained on a GEMINI LEO 1530VP field emission microscope with associated energy dispersive spectroscopy (EDS) and all $CaCO_3$ samples were Pt-coated prior to the SEM examination. X-ray diffraction (XRD) patterns were recorded on a Shimadzu XD-3A instrument with Cu Kα radiation ($\lambda = 1.5418$ Å) at room temperature. Thermogravimetric analysis (TGA) was performed on a Perkin–Elmer TGA-7 instrument, samples were heated at 20 °C/min from room temperature to 800 °C in nitrogen atmosphere. Dynamic laser scattering (DLS) measurements were performed using a Brookhaven laser light scattering spectrometer (BI-200SM) equipped with a digital detector (BI-PAD) and a semiconductor laser light source operating at 532 nm.

2.3. Syntheses

2.3.1. Benzylidene-2,2-bis(oxymethyl) propionic anhydride (Bn-BMPA-Ah)

As shown in Scheme 1, benzylidene acetal of BMPA (Bn-BMPA) was readily synthesized according to literature [49]. In a typical synthesis, benzaldehyde 24.70 g, BMPA 30.04 g, and a catalyst amount of *p*-TSA were mixed in a glass container and set aside for three days, then aqueous $NaHCO_3$ was added, the raw acetal product was obtained after washing with diethyl ether, acidification and filtration. After recrystallization from acetone pure white crystals of Bn-BMPA 35.72 g, yield 68% was obtained.

Bn-BMPA (17.12 g, 77 mmol) and DCC (9.57 g, 46 mmol) were mixed in 130 mL CH_2Cl_2 and stirred overnight at room temperature. The precipitated byproduct *N*,*N*′-dicyclohexylurea (DCU) was filtered off and washed with a small volume of

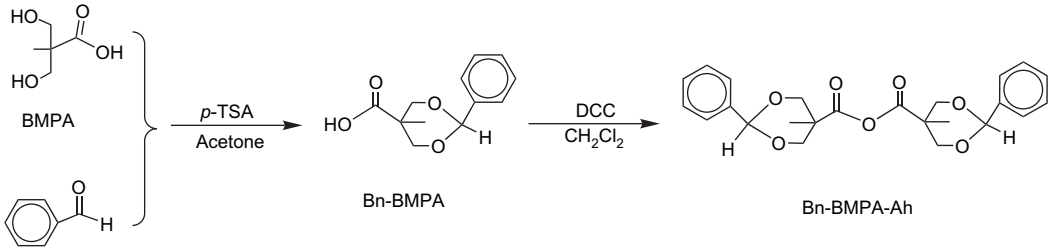

Scheme 1. Synthesis of benzylidene-protected anhydride Bn-BMPA-Ah.

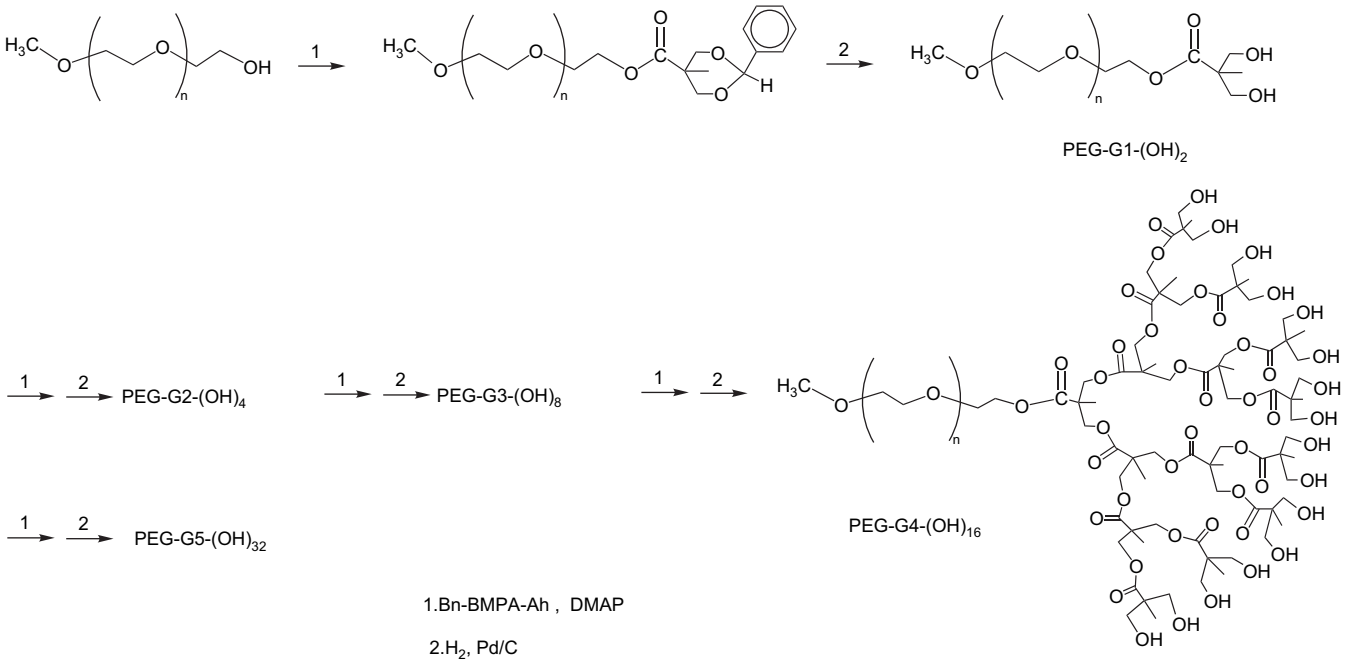

Scheme 2. Synthesis routes for hydroxyl-terminated LDBCs with dendron generations 1–5.

CH_2Cl_2. The filtrate was then precipitated in 800 mL of hexane under vigorous stirring. After filtration and drying 14.69 g Bn-BMPA-Ah was obtained as white powders, yield 89%. ^{1}H NMR (300 MHz, $CDCl_3$, δ in ppm): 1.13 (s, 6H, $-CH_3$), 3.69 (d, 4H, $J = 10.8$ Hz, $-OCH_2C$), 4.68 (d, 4H, $J = 11.4$ Hz, $-OCH_2C$), 5.48 (s, 2H, $ArCHO_2-$), 7.34 (m, 6H, Ar*H*), 7.45 (m, 4H, Ar*H*).

2.3.2. LDBCs of variant dendron generations with hydroxyl terminal groups

A simple and highly efficient divergent approach for the synthesis of aliphatic ester dendrons through anhydride coupling and hydrogenolysis decoupling protocol reported by Fréchet and coworkers [50] was adopted as shown in Scheme 2. Monohydroxyl linear polymer MPEG was used as the initial core molecule and BMPA as the repeating unit. The hybrid block copolymer of dendron generation *n* (G*n*) before and after carboxylation was denoted as PEG-G*n*-OH and PEG-G*n*-COOH, respectively.

2.3.2.1. General procedure for esterification through anhydride coupling: PEG-G2-(O_2Bn)$_2$. The synthesized first generation PEG-G1-$(OH)_2$ (12.04 g, 2.34 mmol) and DMAP (0.64 g, 5.24 mmol) were dissolved in 30 mL CH_2Cl_2, then four times excess of Bn-BMPA-Ah (7.89 g, 18.51 mmol) was added based on the terminal hydroxyl groups. After stirring at room temperature for 14 h, 5 mL of methanol was added to quench the unreacted Bn-BMPA-Ah. The mixture was stirred for another 8 h and precipitated into diethyl ether, then filtered and washed completely with ether for several times, the solid products were dried in vacuum oven to obtain white powder, 11.43 g, yield 89%. FTIR (KBr, cm^{-1}): 2887 (ν_{C-H}), 1740 ($\nu_{C=O}$), 1525 (ν_{Ar}), 1114 (ν_{C-O}), 746, 700 (γ_{ArC-H}). ^{1}H NMR (300 MHz, $CDCl_3$, δ in ppm): 0.93 (s, 6H, $-CH_3$), 1.25 (s, 3H, $-CH_3$), 3.36 (s, 3H, $-OCH_3$), 3.65 (bs, ~470H, $-OCH_2$), 3.87 (t, 2H, $J = 4.8$ Hz, $-CH_2OCO$), 4.11(t, 2H, $J = 4.8$ Hz, $-CH_2OCO$), 4.39 (s, 4H, $-CH_2OCO$), 4.55 (d, 4H, $J = 11.4$ Hz, $-CH_2OCO$), 5.40 (s, 2H, $ArCHO_2-$), 7.30 (m, 6H, Ar*H*), 7.38 (m, 4H, Ar*H*).

2.3.2.2. General deprotection procedure of the benzylidene groups: PEG-G2-$(OH)_4$. Removal of the benzylidene protecting groups was achieved by catalytic hydrogenolysis. PEG-G2-$(O_2Bn)_2$ (10.54 g, 1.90 mmol) was dissolved in 45 mL 1:2 mixture solvent of CH_2Cl_2/MeOH in a glass flask, and then 0.95 g of 10 wt% Pd/C catalyst was added. The mixture was stirred vigorously for 2–3 days under H_2 at atmospheric pressure. After removal of catalyst by filtration, the filtrate was precipitated in diethyl ether to give the second generation product of PEG-G2-$(OH)_4$, 9.66 g, yield 94%. FTIR (KBr, cm^{-1}): 3594 (ν_{O-H}), 2887 (ν_{C-H}), 1740 ($\nu_{C=O}$), 1114 (ν_{C-O}). ^{1}H NMR (300 MHz, $CDCl_3$, δ in ppm): 1.09 (s, 6H, $-CH_3$), 1.31 (s, 3H, $-CH_3$), 3.31 (s, $-OH$), 3.38 (s, 3H, $-OCH_3$), 3.65 (bs, ~460H, $-OCH_2$), 3.89 (m, 8H, $-CH_2OH$), 4.32 (m, 4H, $-CH_2OCO$), 4.40 (d, 2H, $J = 10.1$ Hz, $-CH_2OCO$).

2.3.2.3. PEG-G3-(O_2Bn)$_4$. PEG-G2-$(OH)_4$ (9.26 g, 1.73 mmol), Bn-BMPA-Ah (11.75 g, 27.58 mmol) and DMAP (0.56 g, 4.57 mmol) were mixed and reacted in 60 mL CH_2Cl_2 according to the general procedure. The product was obtained by precipitating the mixture into diethyl ether to give white product of PEG-G3-$(O_2Bn)_4$, 10.13 g, yield 94%. FTIR (KBr, cm^{-1}): 2887 (ν_{C-H}), 1740 ($\nu_{C=O}$), 1520 (ν_{Ar}), 1114 (ν_{C-O}), 746, 701 (γ_{ArC-H}). ^{1}H NMR (300 MHz, $CDCl_3$, δ in ppm): 0.92 (s, 12H, $-CH_3$), 1.08 (s, 6H, $-CH_3$), 1.2 (s, 3H, $-CH_3$), 3.36 (s, 3H, $-OCH_3$), 3.65 (bs, ~470H, $-OCH_2$), 3.87 (t, 2H, $J = 4.8$ Hz, $-CH_2OC$), 4.06 (d, 4H, $J = 5.1$ Hz, $-CH_2OCO$), 4.17 (t, 2H, $J = 4.8$ Hz, $-CH_2OCO$), 4.34 (m, 8H, $-CH_2OCO$),

4.60 (q, 8H, $J = 11.4$ Hz, $-CH_2OCO$), 5.40 (s, 4H, $ArCHO_2-$), 7.31 (m, 12H, Ar*H*), 7.45 (m, 8H, Ar*H*).

2.3.2.4. PEG-G3-(OH)$_8$. PEG-G3-$(O_2Bn)_4$ (9.61 g, 1.56 mmol), Pd/C (0.84 g) were allowed to react in 40 mL mixture solvent according to the general procedure. After removal of catalyst by filtration, the filtrate was precipitated in diethyl ether to give PEG-G3-$(OH)_8$, 7.85 g, yield 87%. FTIR (KBr, cm^{-1}): 3507 (ν_{O-H}), 2887 (ν_{C-H}), 1739 ($\nu_{C=O}$), 1114 (ν_{C-O}). ^{1}H NMR (300 MHz, $CDCl_3$, δ in ppm): 1.03 (s, 12H, $-CH_3$), 1.23 (s, 9H, $-CH_3$), 3.23 (s, $-OH$), 3.33 (s, 3H, $-OCH_3$), 3.59 (bs, ~460H, $-OCH_2$), 3.73–3.82 (m, 16H, $-CH_2OH$), 4.23 (m, 14H, $-CH_2OCO$).

2.3.2.5. PEG-G4-(O$_2$Bn)$_8$. PEG-G3-$(OH)_8$ (6.84 g, 1.18 mmol), Bn-BMPA-Ah (15.98 g, 37.51 mmol), DMAP (0.93 g, 7.62 mmol) and 60 mL CH_2Cl_2 were reacted according to the general procedure. The product was obtained by precipitating the mixture into diethyl ether to give white product of PEG-G4-$(O_2Bn)_8$, 8.31 g, yield 95%. FTIR (KBr, cm^{-1}): 2887(ν_{C-H}), 1740 ($\nu_{C=O}$), 1510 (ν_{Ar}), 1113 (ν_{C-O}), 746, 700 (δ_{ArC-H}). ^{1}H NMR (300 MHz, $CDCl_3$, δ in ppm): 0.90 (s, 24H, $-CH_3$), 1.07 (s, 12H, $-CH_3$), 1.14 (s, 3H, $-CH_3$), 1.18 (s, 6H, $-CH_3$), 3.37 (s, 3H, $-OCH_3$), 3.65 (bs, ~470H, $-OCH_2$), 3.87 (t, 2H, $J = 4.8$ Hz, $-CH_2OCO$), 4.04 (s, 4H, $-CH_2OCO$), 4.15 (m, 8H, $-CH_2OCO$), 4.33 (m, 16H, $-CH_2OCO$), 4.55 (d, 16H, $J = 11.1$ Hz, $-CH_2OCO$), 5.38 (s, 8H, $ArCHO_2-$), 7.30 (m, 24H, Ar*H*), 7.38 (m, 16H, Ar*H*).

2.3.2.6. PEG-G4-(OH)$_{16}$. PEG-G4-$(O_2Bn)_8$ (8.23 g, 1.11 mmol), 0.80 g Pd/C and 50 mL mixture solvent were reacted according to the general procedure under H_2 atmosphere. After removal of catalyst by filtration, the filtrate was precipitated in diethyl ether to give PEG-G4-$(OH)_{16}$ 5.31 g, yield 71%. FTIR (KBr, cm^{-1}): 3404 (ν_{O-H}), 2889 (ν_{C-H}), 1728 ($\nu_{C=O}$), 1115 (ν_{C-O}). ^{1}H NMR (300 MHz, acetone-d_6, δ in ppm): 1.13 (s, 24H, $-CH_3$), 1.32 (m, 21H,$-CH_3$), 3.00 (s, $-OH$), 3.31 (s, 3H, $-OCH_3$), 3.60 (bs, ~460H, $-OCH_2$), 3.70–3.82 (m, 32H, $-CH_2OH$), 4.32 (t, 28H, $J = 11.1$ Hz, $-CH_2OCO$).

2.3.2.7. PEG-G5-(O$_2$Bn)$_{16}$. PEG-G4-$(OH)_{16}$ (2.78 g, 0.42 mmol), Bn-BMPA-Ah (10.58 g, 24.84 mmol) and DMAP (0.73 g, 6.01 mmol) were reacted in 35 mL CH_2Cl_2 according to the general procedure. The product was obtained by precipitating the mixture into diethyl ether to give white product of PEG-G5-$(O_2Bn)_{16}$ 3.95 g, yield 88%. FTIR (KBr, cm^{-1}): 2887 (ν_{C-H}), 1740 ($\nu_{C=O}$), 1526 (ν_{Ar}), 1114 (ν_{C-O}), 747, 700 (γ_{ArC-H}). ^{1}H NMR (300 MHz, acetone-d_6, δ in ppm): 0.86 (s, 48H, $-CH_3$), 0.90–1.10 (m, 21H, $-CH_3$), 1.16 (s, 24H, $-CH_3$), 3.36 (s, 3H, $-OCH_3$), 3.65 (bs, ~480H, $-OCH_2$), 3.87 (t, 4H, $J = 4.8$ Hz, $-CH_2OC$), 4.03 (m, 32H, $-CH_2OCO$), 4.31 (s, 32H, $-CH_2OCO$), 4.50 (d, 32H, $J = 11.4$ Hz, $-CH_2OCO$), 5.35 (s, 16H, $ArCHO_2-$), 7.27 (m, 48H, Ar*H*), 7.35 (m, 32H, Ar*H*).

2.3.2.8. PEG-G5-(OH)$_{32}$. PEG-G5-$(O_2Bn)_{16}$ (3.86 g, 0.36 mmol), 0.394 g Pd/C and 30 mL mixture solvent were reacted according to the general procedure under H_2 atmosphere. After removal of catalyst by filtration, the filtrate was precipitated in diethyl ether to give PEG-G5-$(OH)_{32}$, 2.32 g, yield 75%. FTIR (KBr, cm^{-1}): 3429 (ν_{O-H}), 2887 (ν_{C-H}), 1740 ($\nu_{C=O}$), 1114 (ν_{C-O}). ^{1}H NMR (300 MHz, acetone-d_6, δ in ppm): 1.06 (s, 48H, $-CH_3$), 1.21 (m, 48H, $-CH_3$), 3.32 (s, 3H, $-OCH_3$), 3.63 (bs, ~470H, $-OCH_2$), 3.70–3.81 (m, 64H, $-CH_2OH$), 4.05–4.47 (m, 60H, $-CH_2OCO$).

2.3.3. Carboxylic acid functionalized LDBCs of variant dendron generations

2.3.3.1. General procedure for carboxylic acid functionalized LDBC: PEG-G4-COOH. The carboxylic acid functionalization of the surface hydroxyl groups was realized by reaction with SA in acetone under optimized conditions [41] as shown in Scheme 3. PEG-G4-$(OH)_{16}$ (1.00 g, 0.15 mmol, 1 eq.) and SA (0.69 g, 7.0 mmol, 2.5 eq.) was mixed in 15 mL acetone in a three-necked flask under N_2 atmosphere. After refluxed for 7 h under stirring, the mixture was precipitated in 250 mL of diethyl ether. The crude product was further purified by exhaustive dialysis against de-ionized water using an osmosis membrane (from Shanghai Greenbird Sci. and Tech. Co.) with a MWCO of 3500 g/mol to remove unreacted small molecules, after drying in a vacuum oven to afford 1.11 g of white product, yield 90%. FTIR (KBr, cm^{-1}): 2890 (ν_{C-H}), 2554 (ν_{COOH}), 1744 ($\nu_{C=O}$), 1111 (ν_{C-O}). ^{1}H NMR (300 MHz, acetone-d_6, δ in ppm): 1.14 (s, 3H, $-CH_3$), 1.34 (m, 42H, $-CH_3$), 2.58–2.62 (m, 56H, $-OOCCH_2CH_2COOH$), 3.60 (bs, ~460H, $-OCH_2$), 3.82 (m, 6H, $-CH_2OH$), 4.32 (m, 58H, $-CH_2OCO$), 9.88 (s,$-COOH$).

2.3.3.2. PEG-G3-COOH. PEG-G3-$(OH)_8$ (0.74 g, 0.12 mmol, 1 eq.) and SA (0.25 g, 2.5 mmol, 2.5 eq.) and 15 mL acetone were mixed and reacted according to the general procedure. The crude mixture was purified to afford 0.76 g of white product, yield 90%. FTIR (KBr, cm^{-1}): 2884 (ν_{C-H}), 2582 (ν_{COOH}), 1742 ($\nu_{C=O}$), 1114 (ν_{C-O}). ^{1}H NMR (300 MHz, acetone-d_6, δ in ppm): 1.21 (m, 21H, $-CH_3$), 2.62 (s, 28H, $-OOCCH_2CH_2$-COOH), 3.36 (s, 3H, $-OCH_3$), 3.59 (bs, ~460H, $-OCH_2$), 3.85 (m, 2H, $-CH_2OH$), 4.21 (m, 28H, $-CH_2OCO$), 9.58 (s, $-COOH$).

2.3.3.3. PEG-G5-COOH. PEG-G5-$(OH)_{32}$ (0.92 g, 0.11 mmol), SA (0.98 g, 9.80 mmol.) and 15 mL acetone were reacted according to the general procedure. The crude mixture was purified to afford 1.14 g of white product, yield 90%. FTIR (KBr, cm^{-1}): 2892 (ν_{C-H}), 2575 (ν_{COOH}), 1740 ($\nu_{C=O}$), 1128 (ν_{C-O}). ^{1}H NMR (300 MHz, acetone-d_6, δ in ppm): 1.13–1.45 (m, 93H, $-CH_3$), 2.60 (s, 116H, $-OOCCH_2CH_2COOH$), 3.39 (s, 3H, $-OCH_3$), 3.59 (bs, ~500H, $-OCH_2$), 4.13–4.5 (m, 104H, $-CH_2OCO$), 11.01 (s,$-COOH$).

2.4. Precipitation of $CaCO_3$ in the presence of functionalized LDBCs

The static precipitation method [22] was employed for the $CaCO_3$ crystallization. Doubly distilled water was used to

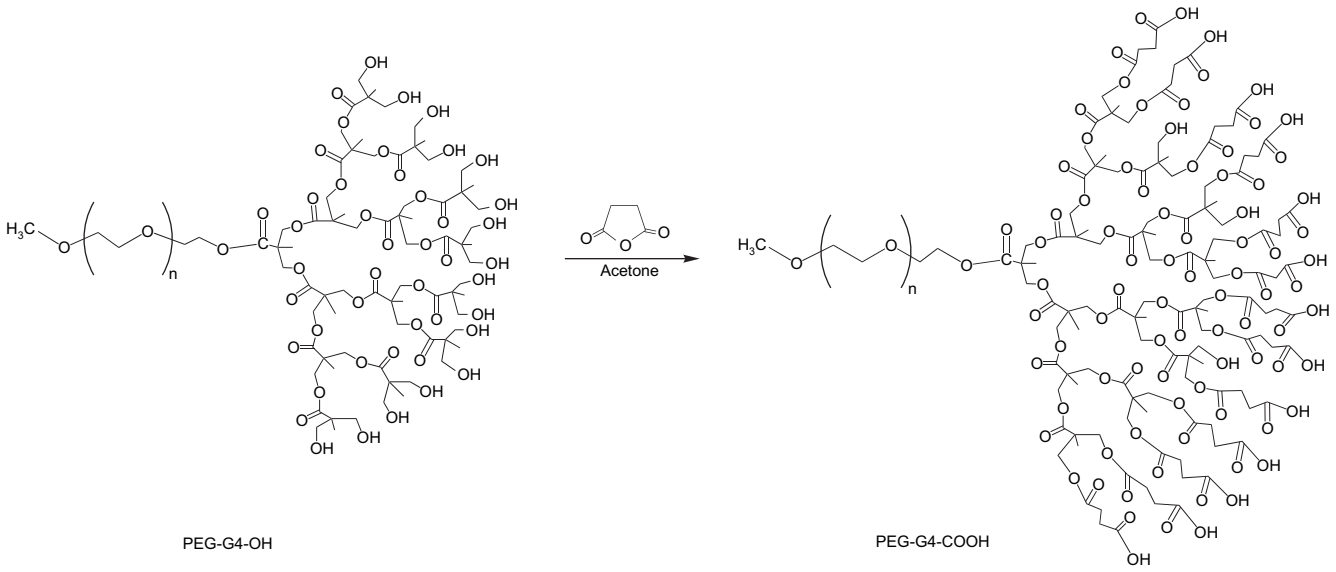

Scheme 3. Carboxylated modification of the fourth generation LDBC.

prepare aqueous $CaCl_2$, $NaHCO_3$ and LDBC additives solutions. The pH of the solutions was adjusted to a desired value before mixing by using HCl or NaOH solution. The crystallization was carried out at 18 °C or a moderate higher temperature 30 °C. In a typical procedure, $CaCl_2$ (20.0 mL, 0.025 M, pH = 10), functionalized LDBC (20.0 mL, 0.8 g/L, pH = 10), and $NaHCO_3$ (20.0 mL, 0.025 M, pH = 10) were added to a glass vessel simultaneously under vigorous stirring. This gave a final $CaCO_3$ concentration of 8.3 mM. After a brief stirring for 1 min, the solution was left to stand for 24 h at 18 °C under static condition. The crystalline $CaCO_3$ was collected by centrifugation and washed twice with distilled water, and then the dried samples were characterized with FTIR, SEM, XRD and TGA analyses.

3. Results and discussion

3.1. Syntheses of LDBCs with carboxylic acid terminal groups

The syntheses of series hydroxyl-terminated LDBCs of PEG-*dendr*(PBMPA) were readily achieved by the divergent protocol reported by Fréchet and coworker [50] as outlined in Scheme 2. Here MPEG was used as the growing core for the divergent approach to synthesize aliphatic polyester dendron segments. This divergent approach mainly composed of anhydride coupling and catalytic hydrogenolysis, for both by-products from the coupling reaction step, the benzylidene-protected acid Bn-BMPA and its methyl ester formed during the coupling and quenching reactions, were readily soluble in diethyl ether, but the LDBCs were not, so after precipitation, filtration and washing with diethyl ether, the highly pure LDBCs were harvested as white powders. The removal of the benzylidene protecting groups was readily achieved by catalytic hydrogenolysis even under atmospheric hydrogen pressure to obtain the hydroxyl-terminated LDBCs. So really that the divergent growth progressed well in a homogeneous medium and required no means of purification other than a simple solvent extraction and precipitation as reported in the literature [50]. On further modification the terminal hydroxyl groups were transformed to functionalized carboxylic acids via ring-opening esterification with SA as representatively shown in Scheme 3. The growth of each dendron generation and the surface group modification was strictly tracked by ^{1}H NMR and FTIR. Generally speaking, the complete deprotection of the benzylidene groups were directly monitored and affirmed by the disappearance of the signals corresponding to the benzylic and aromatic protons at about 5.4 and 7.25–7.45 ppm, respectively, in the ^{1}H NMR spectra and the phenyl ring skeleton stretching around 1520 cm^{-1} and aromatic C–H bending at 746 and 700 cm^{-1} in the FTIR spectra. At most time the proton signal of the active hydroxyl and carboxylic acid could be seen as a broader singlet at about 3.0 and 9.6–11 ppm, respectively, which could be confirmed by its disappearance with the addition of droplets of deuterated water. As for the step-growth dendritic block, the same group resonance varied at different layers and shifted downfield for the successive generational layers because of the steric hindrance effect [50,51]. For instance, Fig. 1 shows the typical ^{1}H NMR spectra comparison of the fourth generation LDBC before and after functionalization with carboxylic acid groups. In Fig. 1a, the methyl resonance peaks are mainly located at around 1.14 and 1.34 ppm for the methyl d groups of surface BMPA units and d′ of interior units, respectively. And similarly the multiple peaks around 3.75 and 4.32 ppm belongs to the surface methylene e linked with hydroxyl groups and the interior methylene f attached with ester groups. The single peak c at 3.3 is assigned to the end methoxy group and the very strong broad single peak around 3.6 ppm to the two methylene groups a and b of linear PEG chain. The singlet g at 3.0 is from the hydroxyl proton which disappears after shaking with the addition of two small drops of D_2O. As shown in Fig. 1b, after carboxylated modification, the appearance of peaks h and i at around 2.6 ppm attributing to the methylene of attached succinic

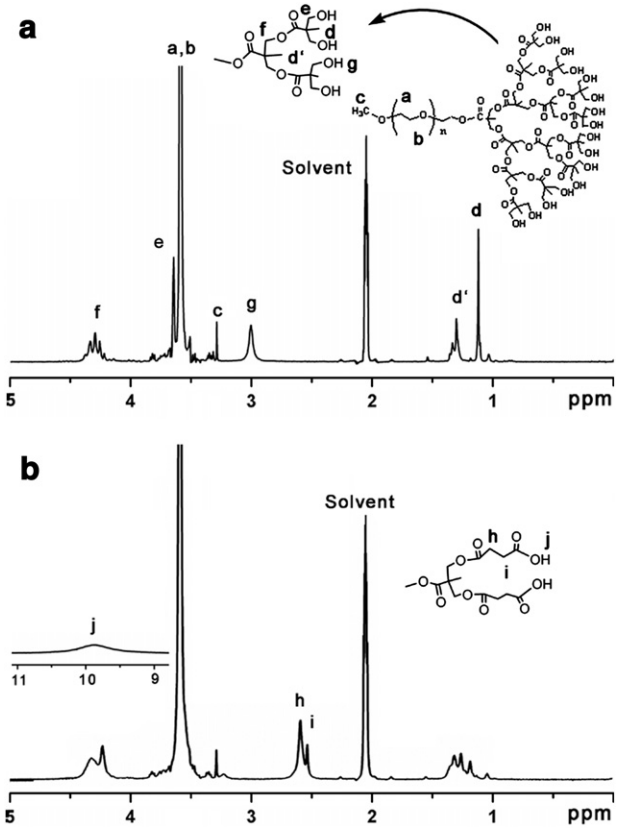

Fig. 1. ^{1}H NMR spectra comparison of the fourth generation LDBC before and after carboxylation (a) PEG-G4-$(OH)_{16}$ vs (b) PEG-G4-$(COOH)_{14}$.

acid and the sharp decrease or almost missing of surface methyl and methylene peaks (d and e) and the corresponding intensity increase of interior peaks, also the carboxylic acid proton broad singlet j at around 9.9 directly revealed the successful realization of the ring-opening esterification and the efficient group transformation from −OH to −COOH.

The degree of carboxylation was further determined quantitatively by titration of terminal carboxylic acid groups, which was in agreement with the estimated results from the peaks integral area ratio of the ^{1}H NMR spectra. The results are summarized in Table 1. More than 85% degree of carboxylation was achieved for all LDBCs showing no dendron generation influence, which was in contrast with the results from hyperbranched polyesters of 60–80% degree of carboxylation exhibiting a remarkable decrease with the increased pseudo-generation [41]. This difference may be ascribed to the obviously easy access of surface hydroxyl groups on the regular dendron segments compared with the randomly distributed ones in the hyperbranched polymers which contain chemically differentiated interior hydroxyl groups and periphery ones [52].

The GPC traces of the LDBCs are shown in Fig. 2 and the molecular weights were calibrated using linear polystyrene (PSt) standards as summarized in Table 2. Although the GPC data provided valuable information about the changing tendency of the sample series and all the hydroxyl-terminated LDBCs displayed a quite smaller polydispersity index ($PDI = M_w/M_n$) less than 1.18 and also the carboxylated LDBCs with that of lower than 1.27, the molecular weights for these products based on linear PSt standards differed remarkably from the theoretical values. This obvious derivation has also been observed in the similar sample series [50,53] and may mainly be attributed to the globular shape adopted by the dendron segments. It is interesting to note that the carboxylated LDBCs exhibited a very small apparent molecular weight

Table 1
Titration measured values of carboxylic acid groups for variant generations carboxylated LDBCs

Carboxylated LDBCs	−COOH theoretical number	−COOH number titrated	Degree of carboxylation (%)
PEG-G3-COOH	8	7	85.0
PEG-G4-COOH	16	14	86.9
PEG-G5-COOH	32	28	86.5

Table 2
GPC data for the LDBCs based on PSt standards

Samples	Theoretical molar mass (g/mol)	GPC		
		M_w	M_n	PDI
MPEG	5000	5890	5360	1.10
PEG-G3-$(OH)_8$	5810	6180	5420	1.14
PEG-G4-$(OH)_{16}$	6740	6470	5490	1.18
PEG-G5-$(OH)_{32}$	8600	6710	5750	1.17
PEG-G3-$(COOH)_7$	6510	6900	5420	1.27
PEG-G4-$(COOH)_{14}$	8140	6740	5530	1.22
PEG-G5-$(COOH)_{28}$	11 400	7050	5690	1.24

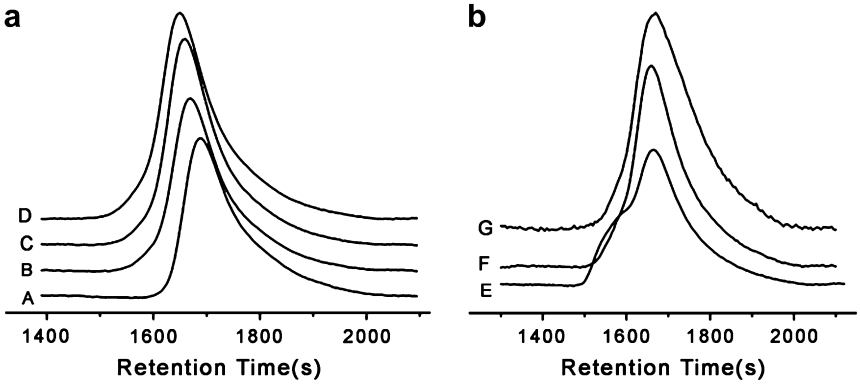

Fig. 2. GPC traces of (a) hydroxyl-terminated LDBCs and (b) carboxylated LDBCs, (A) MPEG, (B) PEG-G3-$(OH)_8$, (C) PEG-G4-$(OH)_{16}$, (D) PEG-G5-$(OH)_{32}$, (E) PEG-G3-$(COOH)_7$, (F) PEG-G4-$(COOH)_{14}$, (G) PEG-G5-$(COOH)_{28}$.

increase compared with their same generation hydroxyl-terminated ones, which was presumably resulted from the more compact conformation due to hydrogen bonding among carboxylic acid groups within the dendritic segment.

3.2. $CaCO_3$ crystallization under the influence of carboxylated LDBCs

3.2.1. Effect of polymer additive LDBC concentrations

The static solution mixing method as reported by Marentette et al. [22] was employed for the precipitation of $CaCO_3$ in the absence and the presence of functionalized LDBCs. Fig. 3 shows the typical SEM micrographs of the produced $CaCO_3$ particles in the presence of various concentrations of the fourth generation carboxylated LDBCs, a $CaCO_3$ concentration of 8.3 mM, a starting pH of 10 and with incubation time 24 h at 18 °C. As shown in Fig. 3a, well-defined rhombohedral crystals characteristic of calcite were obtained without any polymer additives. Meanwhile, mixed morphologies of residual rhombohedral particles and spherical $CaCO_3$ particles of relative wider size distribution with a mean diameter of 0.98 ± 0.18 μm were obtained under the influence of the lowest additive concentration of 0.027 g/L of carboxylated LDBCs as shown in Fig. 3b. Under higher concentrations of

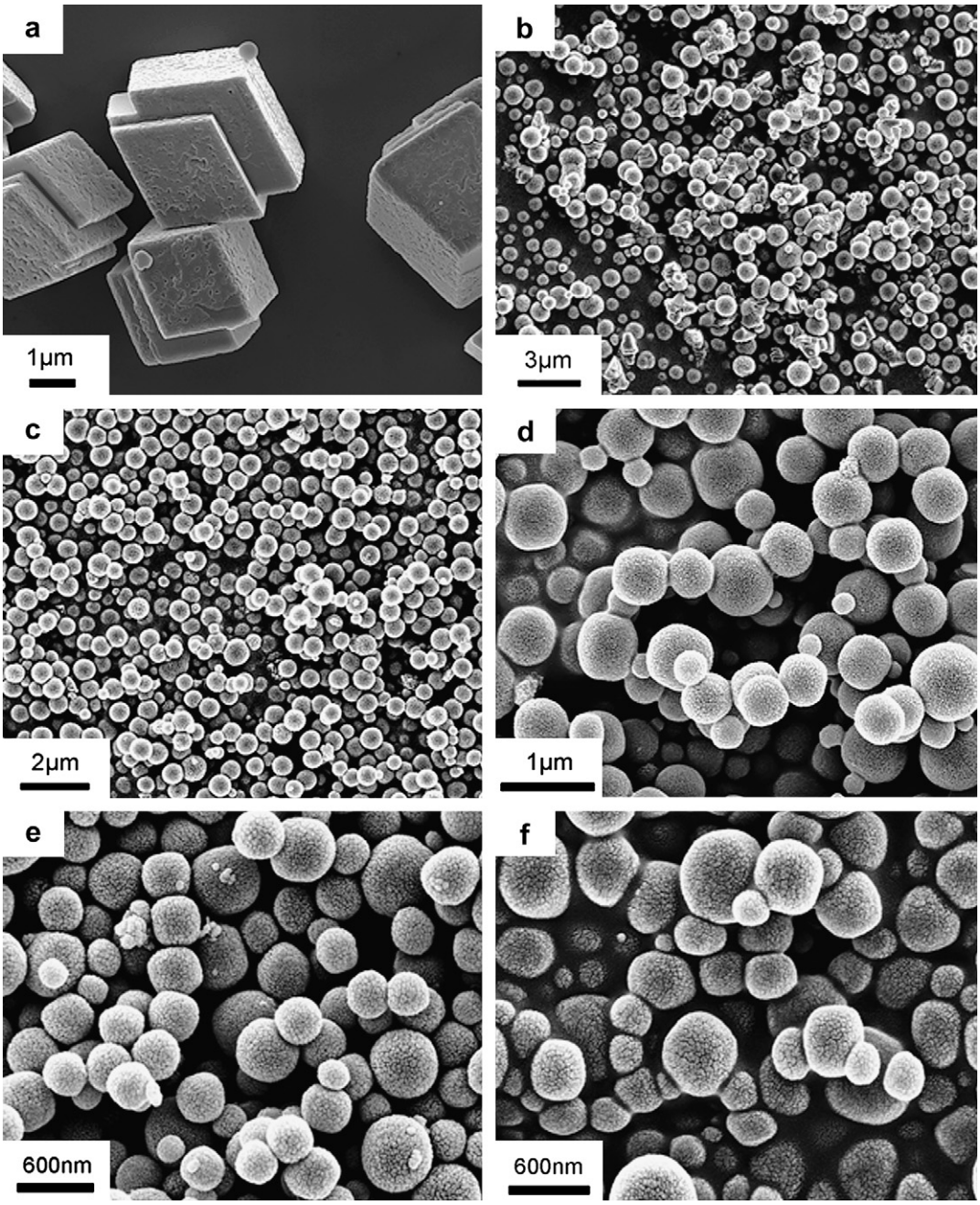

Fig. 3. SEM images of $CaCO_3$ particles obtained at initial pH = 10, $[CaCO_3] = 8.3$ mM, and with incubation time 24 h at 18 °C, (a) in absence of polymeric additives, and in the presence of PEG-G4-$(COOH)_{14}$ at (b) 0.027 g/L, (c) 0.067 g/L, (d) 0.13 g/L, (e) 0.20 g/L, (f) 0.27 g/L.

Table 3
$CaCO_3$ particles obtained under various additive PEG-G4-$(COOH)_{14}$ concentrations at 18 °C

Concentration g/L	Morphology	Sphere diameter[a] (μm)	Polymorphism[b]	
			FTIR	XRD
0.027	Spherical + residual rhombohedral	0.98 ± 0.18	90% v, 10% c	77% v, 23% c
0.067	Spherical	0.60 ± 0.06	100% v	100% v
0.13	Spherical	0.52 ± 0.12	100% v	100% v
0.20	Spherical	0.41 ± 0.07	100% v	100% v
0.27	Spherical	0.42 ± 0.11	100% v	100% v

v, Vaterite; c, calcite.
[a] Over 80 typical particles were measured from SEM pictures for each sample group.
[b] From FTIR and XRD quantitative analyses.

LDBCs, mainly spherical $CaCO_3$ particles with reduced sizes were produced as shown in Fig. 3c–f. These spherical particles were of typical morphology for vaterite polymorph [41] and confirmed by FTIR and XRD analyses. FTIR quantitative analyses of the bands at 745 and 712 cm^{-1} characteristic of vaterite and calcite polymorphs, respectively [54], indicated the high content vaterite formation (Table 3). As shown in Fig. 4, the crystal phases of produced $CaCO_3$ were further analyzed by XRD, the results affirmed that the particles were made up of vaterite and calcite polymorphs and the vaterite contents calculated by Rao's equation agreed well with that from FTIR quantitative analysis (also see Table 4) except for the lowest concentration 0.027 g/L sample, the significant deviation may come from the analysis sample preparation, carefulness was required for the FTIR quantitative analysis [41,54]. SEM coupled with energy dispersive X-ray spectrometer has been used to determine the elemental composition of individual particles [55]. Although the experimental solutions contained NaCl, the EDS results of different precipitated particles with variant morphologies verified that all the produced powder materials were $CaCO_3$ without the presence of Na (1.0 keV) and Cl (2.6 keV) or other contaminants as representatively shown in Fig. 5 for the sample from 0.067 g/L G4 carboxylated polymer additive solutions. The Pt peaks were from the sputtered platinum coating during SEM sample preparation, Ca (3.7, 4.0 keV), C (0.28 keV) and O (0.53 keV) confirmed the $CaCO_3$ composition and the relatively higher carbon content presumably indicated the presence of strongly associated polymer additives even after extensive washing [56], which was also verified by the TGA results. The LDBC additive exhibited so strong vaterite polymorph selectivity that even under quite low concentration of 0.067 g/L, essentially pure vaterite (100% by FTIR and XRD) spherical crystals with diameter of 0.60 ± 0.06 μm was obtained. A further increase of the additive concentration to 0.13 and 0.20 g/L, pure vaterite spherical particles were produced with monotonically decreased diameters of 0.52 ± 0.12 and 0.41 ± 0.07 μm, respectively. While further increasing the additive concentration, the spherical vaterite particle size leveled off, for instance, particles with a diameter of 0.42 ± 0.11 μm were achieved with carboxylated LDBC concentration of 0.27 g/L (Table 3), which might imply a saturated additive concentration for the crystallization modification.

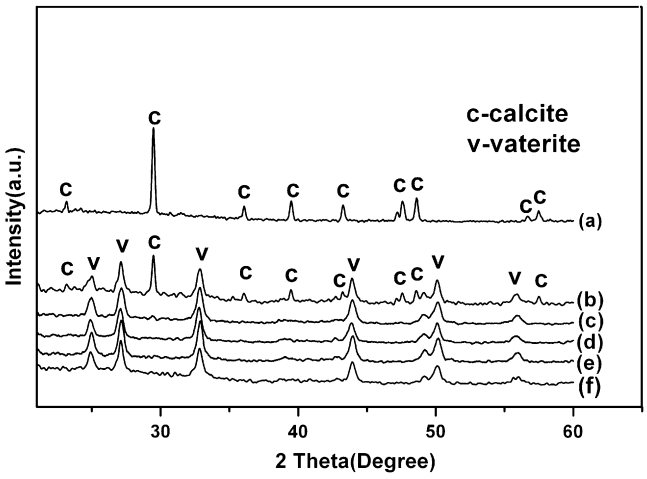

Fig. 4. XRD patterns of $CaCO_3$ particles obtained at the same conditions as in Fig. 3.

3.2.2. Effect of dendritic segment generation number of carboxylated LDBCs with the same mass concentration of polymer additives

Fig. 6 shows the morphologies of thus obtained $CaCO_3$ particles by changing the dendritic segment generation number

Table 4
$CaCO_3$ particles obtained at 30 °C

Polymer additive	Mass concentration (g/L)	[$-COO^-$] (mM)	Morphology	Sphere diameter[a] (μm)	Polymorphism[b]	
					FTIR	XRD
PEG-G3-$(COOH)_7$	0.35	0.375	Spherical + stacked rhombohedral	1.18 ± 0.21	92% v, 8% c	92% v, 8% c
PEG-G4-$(COOH)_{14}$	0.22	0.375	Spherical + pine-cone shaped	1.07 ± 0.13	90% v, 10% c	90% v, 10% c
PEG-G5-$(COOH)_{28}$	0.15	0.375	Spherical + pine-cone shaped	0.98 ± 0.10	95% v, 5% c	96% v, 4% c

Initial pH = 10, [CaCO3] = 8.3 mM, and in the same molar concentration of carboxylic acid functional group; v, vaterite; c, calcite.
[a] Over 80 typical particles were measured from SEM pictures for each sample group.
[b] From FTIR and XRD quantitative analyses.

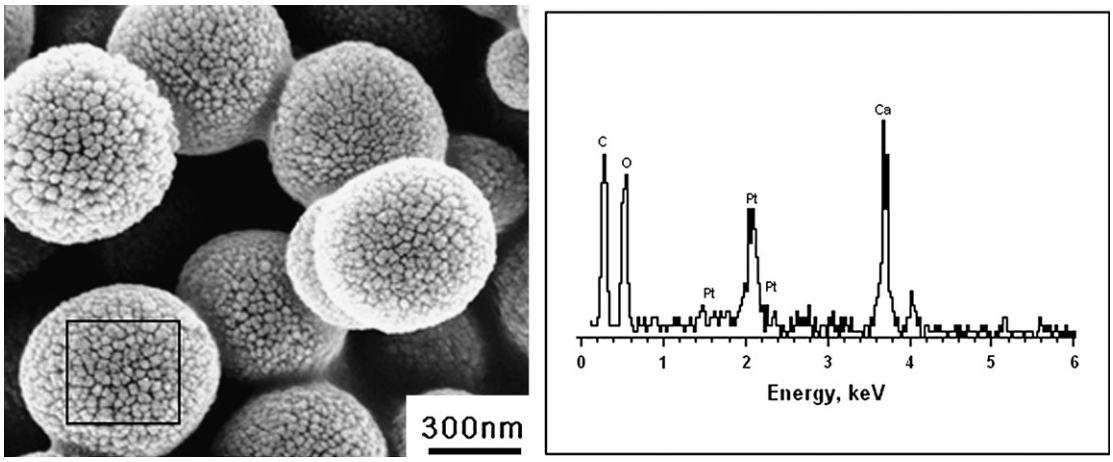

Fig. 5. The representative energy dispersive X-ray spectrum of the single particle analysis for the $CaCO_3$ sample from 0.067 g/L PEG-G4-$(COOH)_{14}$ at the same condition as in Fig. 3c, the marked particle is the one selected for EDS analysis.

with fixed mass concentration 0.27 g/L of polymer additives. Although essentially 100% vaterite spheres were obtained from FTIR and XRD analyses, the diameters of produced particles statistically measured from SEM images were 0.51 ± 0.05, 0.42 ± 0.11, 0.29 ± 0.06 μm for dendritic segment G3, G4 and G5, respectively, decreased monotonically with increasing generation number. The surface of the vaterite spheres obtained from G3 modifier was significantly rougher than that from G4 and G5. Close inspections disclosed that these spheres were aggregates of nanocrystallites of 90 nm for G3, 50 nm for G4 and 40 nm for G5 (Fig. 6b,d and f). This kind of narrow distributed or monodisperse spherical assembly from nanoparticle microspheres has also been recently reported from polypeptide stabilized $CaCO_3$ nanoparticles [57].

The polymer additive organic components of 1.79, 5.65 and 11.9 wt% were found by TGA analysis from the $CaCO_3$ particles obtained in the presence of 0.27 g/L of carboxylated LDBCs of G3, G4 and G5, which corresponds to the samples shown in Fig. 6a,c and e, respectively. The significant increase of incorporated polymer additives with increasing generation number revealed the promoted binding efficiency and stronger adsorption ability for higher generation carboxylated LDBCs, which also accounted for the enhanced polymorph and morphology control ability.

3.2.3. Effect of mineralization temperature and dendritic segment generation number of carboxylated LDBCs with the same molar concentration of terminal carboxylic acid groups

A series of $CaCO_3$ products were obtained in the presence of variant generation LDBCs with the same molar concentration of carboxylic acid functional group of 0.375 mM at a higher mineralization temperature 30 °C. The corresponding mass concentrations for carboxylated LDBCs of G3, G4 and G5 were 0.35, 0.22 and 0.15 g/L, respectively. It is interesting to note that the $CaCO_3$ crystals obtained at this higher temperature 30 °C were mixture of calcite and vaterite both from FTIR and XRD analyses as summarized in Table 4, moreover, the diameters of the vaterite spheres of around 1 μm based on SEM characterization (Table 4) were twice more larger than those obtained at lower temperature 18 °C. A higher supersaturation and faster crystallization growth rate associated with the higher mineralization temperature accounted for the generation of significantly larger vaterite spheres and partly loss of the biomimetic stability of metastable vaterite and formation of thermodynamically stable calcite crystals. It should be noted that in our contrast experiments in the presence of hydroxyl-terminated LDBCs only calcite polymorph was obtained almost the same as no-additive control sample. So the same level size particles obtained under the same molar concentration of carboxylic acid manifested the predominant role of the functional group, meanwhile, the slight decrease of the spherical vaterite diameters with increasing generation number also indicated the moderate influence of the architectural structure of variant generations. Therefore, for the combination of linear and functionalized dendritic blocks, LDBCs performed better crystallization inhibition especially much stronger vaterite polymorph selectivity compared with linear DHBCs [23], moreover, they exhibited more diverse morphology control ability under variant conditions and could obtain nearly monodisperse submicrometer vaterite spheres compared with that ranged from 5.8 ± 1.8 to 1.5 ± 0.6 μm got from variant generations of PAMAM dendrimers [37]. Furthermore, it is surprising that the pine-cone shaped calcite were formed in the presence of G4 and G5 LDBCs (Fig. 7c–f and insets), while only few stacked rhombohedral crystals were obtained under G3 LDBCs (Fig. 7a,b and the inset), the dendron generation dependent morphology change is reminiscent of special morphogenesis due to selective adsorption of variable DHBC functional block length [58]. The pine-cone shaped calcite aggregates were on average 1.5 and 0.8 μm in the long and short axes. This kind of pine-cone shaped $CaCO_3$ particles were ever reported to form under the joint influence of linear double hydrophilic block copolymer PEO-*b*-PMAA and surfactant cetyltrimethylammonium bromide (CTAB) [59]. Thus the carboxylic acid functionalized LDBCs of G4 and G5 behaved very similarly as the PEO-*b*-PMAA/CTAB complex, which indicated their amphiphilic character and the formation

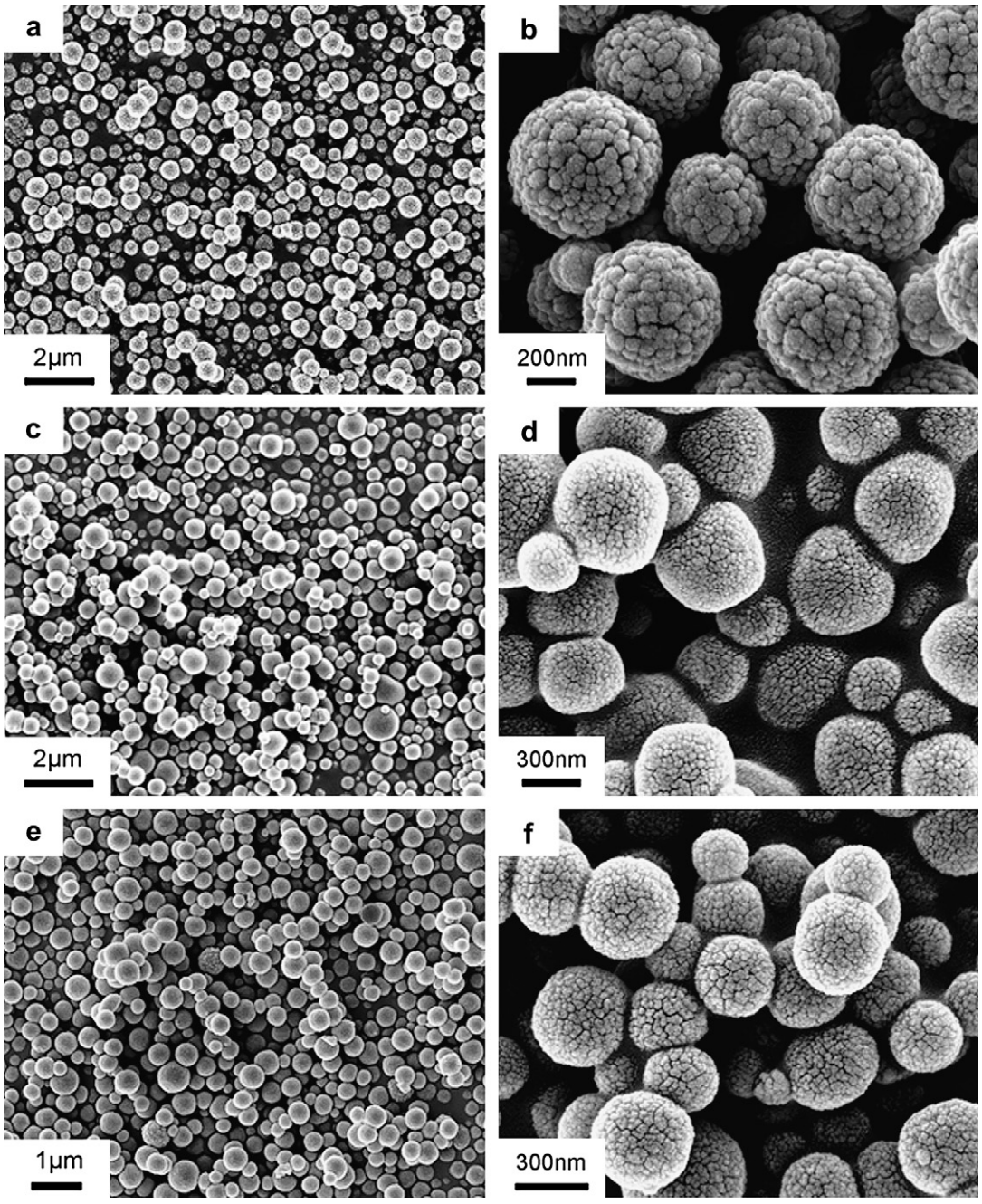

Fig. 6. SEM images of $CaCO_3$ particles obtained at 18 °C with initial pH 10, and in the presence of 0.27 g/L LDBC additives of (a,b) PEG-G3-$(COOH)_7$, (c,d) PEG-G4-$(COOH)_{14}$, (e,f) PEG-G5-$(COOH)_{28}$, (b,d,f) high-magnification SEM images.

of some kind aggregates in the aqueous solution and implied some common mechanism on the modification of $CaCO_3$ mineralization. We performed dynamic laser scattering (DLS) to study the solution properties of carboxylated LDBCs and their mixtures with metal ions, the preliminary results confirmed the presence of large aggregates in the carboxylated LDBCs aqueous solution and their adaptive size increase when reacted with calcium ions which might afford a key clue for the mineralization modification mechanism. For instance, the aggregate particle size for the PEG-G4-$(COOH)_{14}$ solution (0.22 g/L, pH 10) was measured to be 99.9 nm, while with the addition of the same volume of $CaCl_2$ solution (0.025 M, pH 10), the average size of the aggregates increased to 160.9 nm. This kind of adaptive construction and enlarging of inorganic structure through perturbing the organic template have been observed in variant systems [60] while in contrast to the star-like core–corona micelle shrinkage of amphiphilic triblock copolymers with their corona segment poly(acrylic acid) interacting with Ca^{2+} [61]. So at present, the energy preferred crystal face selective adsorption and polymeric template mechanism which emphasize both the match of crystal unit motifs to spatial patterns of functional groups and the formation of three-dimensional superstructures in the presence of growing crystals proposed for DHBCs [6,23,58] are also believed to take

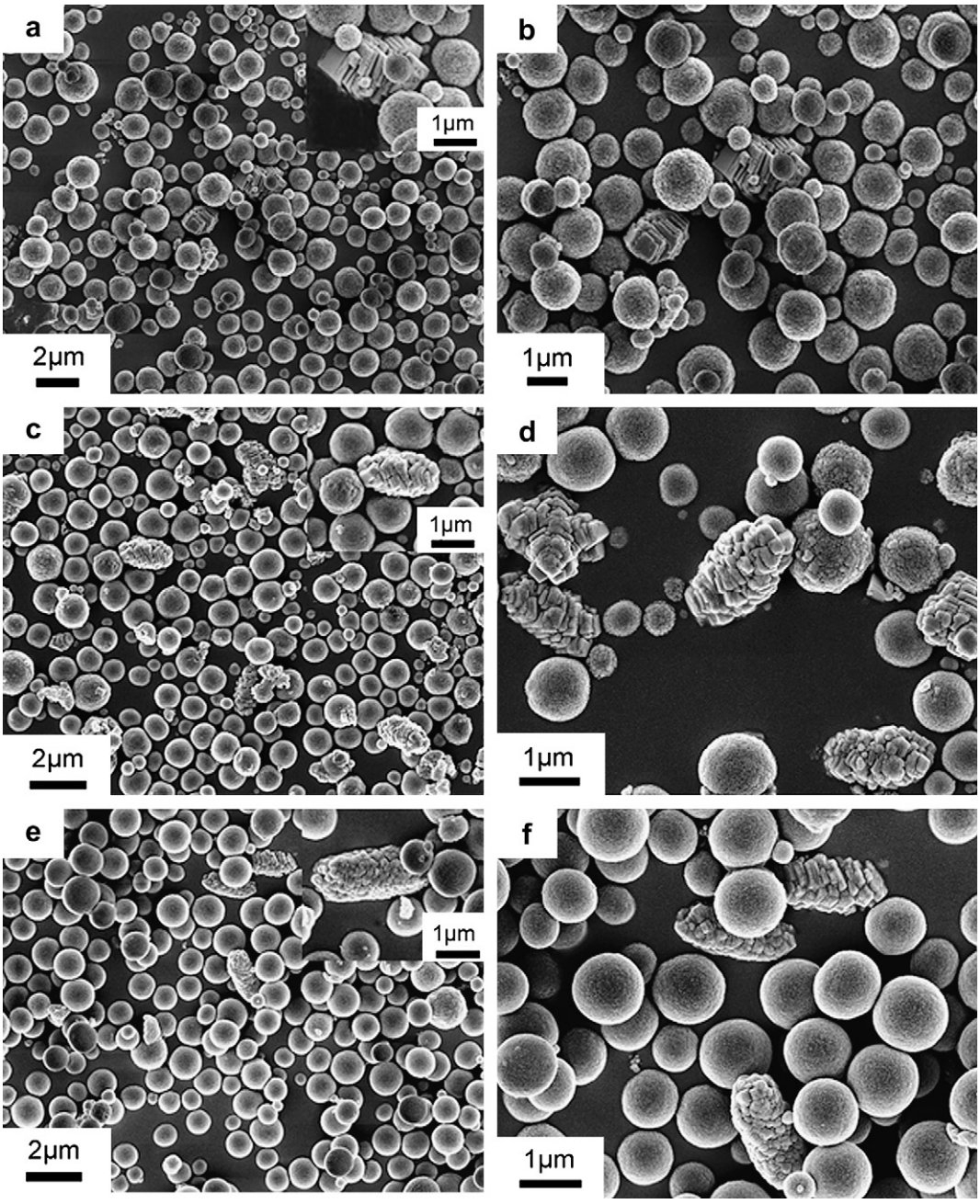

Fig. 7. SEM images of $CaCO_3$ particles obtained at 30 °C, initial pH = 10, $[CaCO_3] = 8.3$ mM, and in the same molar concentration of carboxylic acid functional group $[COO^-] = 0.375$ mM, with (a,b) 0.35 g/L PEG-G3-$(COOH)_7$, (c,d) 0.22 g/L PEG-G4-$(COOH)_{14}$, and (e,f) 0.15 g/L PEG-G5-$(COOH)_{28}$, (b,d,f) high-magnification SEM images.

predominant effect in the LDBCs system, in addition to their spherical conformation and amphiphilic character with increasing dendritic segment generation. The systematic investigation of the carboxylated LDBCs on the biomimetic modification of $CaCO_3$ and their detailed interaction mechanism is currently in progress by a precisely controlled gas diffusion slow crystallization precipitation technique [57,58,62].

4. Conclusions

A series of hybrid block copolymers derived from MPEG and variant generation dendrons from BMPA were synthesized according to a facile divergent strategy, then the hydroxyl groups were successfully transformed into carboxylic acid functional groups with more than 85% conversion efficiency through ring-opening esterification with succinic anhydride. The carboxylated LDBCs thus obtained were employed as $CaCO_3$ crystallization growth modifiers under mild conditions. Mainly spherical $CaCO_3$ particles of gradually reduced sizes were produced with the increase of the polymer additive concentration. With fixed mass concentration of polymer additives, the diameters of produced $CaCO_3$ particles decreased monotonically from 0.51 to 0.42 then 0.29 μm with increasing dendritic segment generation number from G3, G4 to G5,

moreover, these submicrometer spheres were found to be composed of vaterite nanocrystallites of 90, 50 and 40 nm in diameter, respectively. The incorporated polymer additive organic components in the produced minerals increased for their promoted binding efficiency and ever enhanced adsorption ability with the increase of functionalized dendritic segment generation number. The higher mineralization temperature resulted in the formation of significant larger particles and partial calcite crystals for the faster crystallization growth rate and higher supersaturation. Under the same molar concentration of carboxylic acid functional group, the same level size particles were obtained which manifested the crucial role of the functional group, meanwhile, the slight decrease of the vaterite diameters with increasing generation number especially the pine-cone shaped calcite crystals formation under the higher generation carboxylated LDBCs also revealed the significant effect of the architectural structure of variant generations. DLS measurements showed some kind of aggregates formation in the carboxylated LDBC aqueous solution and their adaptive size increase when interacted with calcium ions which may account for the particular pine-cone shaped calcite morphology generation.

Acknowledgements

This work is supported by National Natural Science Foundation of China (NSFC No.50273013), NFFTBS (J0630425), JLMC-YY2007604 and the Scientific Research Foundation for the Returned Overseas Chinese Scholars.

References

[1] Lowenstam HA, Weiner S. On biomineralization. Oxford: Oxford University Press; 1989.
[2] Mann S. Biomimetic materials chemistry. Weinheim: VCH; 1996.
[3] Vincent JFV, Currey JD, editors. The mechanical properties of biological materials. Cambridge, UK: Cambridge University Press; 1980.
[4] Currey JD, Kohn AJ. J Mater Sci 1976;11:1615–23.
[5] Kato T, Sugawara A, Hosoda N. Adv Mater 2002;14:869–77.
[6] Yu SH, Cölfen H. J Mater Chem 2004;14:2124–47.
[7] Cölfen H. Top Curr Chem 2007;271:1–77.
[8] Yu SH. Top Curr Chem 2007;271:79–118.
[9] Xu AW, Ma YR, Cölfen H. J Mater Chem 2007;17:415–49.
[10] Mann S, Heywood BR, Rajam S, Birchall JD. Nature 1988;334:692–5.
[11] Ahn DJ, Berman A, Charych D. J Phys Chem 1996;100:12455–61.
[12] Lahiri J, Xu G, Dabbs DM, Yao N, Aksay IA, Groves JT. J Am Chem Soc 1997;119:5449–50.
[13] Küther J, Nelles G, Seshadri R, Schaub M, Butt HJ, Tremel W. Chem Eur J 1998;4:1834–42.
[14] Küther J, Seshadri R, Nelles G, Butt HJ, Knoll W, Tremel W. Adv Mater 1998;10:401–4.
[15] Aizenberg J, Black AJ, Whitesides GM. J Am Chem Soc 1999;12:4500–9.
[16] Chen BD, Cillliers JJ, Davey RJ, Garside J, Woodburn ET. J Am Chem Soc 1998;120:1625–6.
[17] Rautaray D, Sinha K, Shankar SS, Adyanthaya SD, Sastry M. Chem Mater 2004;16:1356–61.
[18] Hirai T, Hariguchi S, Komasawa I, Davey RJ. Langmuir 1997;13:6650–3.
[19] Walsh D, Lebeau B, Mann S. Adv Mater 1999;11:324–8.
[20] Grassmann O, Löbmann P. Chem Eur J 2003;9:1310–6.
[21] Grassmann O, Löbmann P. Biomater 2004;25:277–82.
[22] Marentette JM, Norwig J, Stockelmann E, Meyer WH, Wegner G. Adv Mater 1997;9:647–51.
[23] Cölfen H, Antonietti M. Langmuir 1998;14:582–9.
[24] Cölfen H, Qi LM. Chem Eur J 2001;7:106–16.
[25] Kaluzynski K, Pretula J, Lapienis G, Basko M, Bartczak Z, Dworak A, et al. J Polym Sci Part A Polym Chem 2001;39:955–63.
[26] Cölfen H. Macromol Rapid Commun 2001;22:219–52.
[27] Chen SF, Yu SH, Wang TX, Jiang J, Cölfen H, Hu B, et al. Adv Mater 2005;17:1461–5.
[28] He LH, Zhang YH, Ren LX, Chen YM, Wei H, Wang DJ. Macromol Chem Phys 2006;207:684–93.
[29] Meng QW, Wang X, Chen DZ, Yu XH. Chin J Inorg Chem 2006;22:447–50.
[30] Kaluzynski K, Pretula J, Penczek S. J Polym Sci Part A Polym Chem 2007;45:90–8.
[31] Kulak AN, Iddon P, Li YT, Armes SP, Cölfen H, Meldrum FC, et al. J Am Chem Soc 2007;129:3729–36.
[32] Levi Y, Albeck S, Brack A, Weiner S, Addadi L. Chem Eur J 1998;4:389–96.
[33] Donners JJJM, Nolte RJM, Sommerdijk NAJM. J Am Chem Soc 2002;124:9700–1.
[34] Estroff LA, Incarvito CD, Hamilton AD. J Am Chem Soc 2004;126:2–3.
[35] Ottaviani MF, Bossmann S, Turro NJ, Tomalia DA. J Am Chem Soc 1994;116:661–71.
[36] Naka K, Tanaka Y, Chujo Y, Ito Y. Chem Commun 1999:1931–2.
[37] Naka K, Tanaka Y, Chujo Y. Langmuir 2002;18:3655–8.
[38] Naka K. Top Curr Chem 2003;228:141–58.
[39] Donners JJJM, Heywood BR, Meijer EW, Nolte RJM, Roman C, Schenning APHJ, et al. Chem Commun 2000:1937–8.
[40] Donners JJJM, Heywood BR, Meijer EW, Nolte RJM, Sommerdijk NAJM. Chem Eur J 2002;8:2561–7.
[41] Meng QW, Chen DZ, Yue LW, Fang JL, Zhao H, Wang LL. Macromol Chem Phys 2007;208:474–84 [cover].
[42] Fréchet JMJ, Gitsov I, Monteil T, Rochat S, Sassi JF, Vergelati C, et al. Chem Mater 1999;11:1267–74.
[43] Choi JS, Lee EJ, Choi YH, Jeong YJ, Park JS. Bioconjugate Chem 1999;10:62–5.
[44] Choi JS, Joo DK, Kim CH, Kim H, Park JS. J Am Chem Soc 2000; 122:474–80.
[45] Wood KC, Little SR, Langer R, Hammond PT. Angew Chem Int Ed 2005;44:6704–8.
[46] Namazi H, Adeli M. Eur Polym J 2003;39:1491–500.
[47] Zhu LY, Zhu GL, Li MZ. Eur Polym J 2002;38:2503–6.
[48] Gillies ER, Jonsson TB, Fréchet JMJ. J Am Chem Soc 2004;126:11936–43.
[49] Annby U, Malmberg M, Pettersson B, Rehnberg N. Tetrahedron Lett 1998;39:3217–20.
[50] Ihre H, De Jesús OLP, Fréchet JMJ. J Am Chem Soc 2001;123:5908–17.
[51] Malkoch M, Malmström E, Hult A. Macromolecules 2002;35:8307–14.
[52] Haag R, Stumbé JF, Sunder A, Frey H, Hebel A. Macromolecules 2000; 33:8158–66.
[53] Carnahan MA, Middleton C, Kim J, Kim T, Grinstaff MW. J Am Chem Soc 2002;124:5291–3.
[54] Vagenas NV, Gatsouli A, Kontoyannis CG. Talanta 2003;59:831–6.
[55] Krueger BJ, Grassian VH, Iedema MJ, Cowin JP, Laskin A. Anal Chem 2003;75:5170–9.
[56] Thachepan S, Li M, Davis SA, Mann S. Chem Mater 2006;18:3557–61.
[57] Zhang ZP, Gao DM, Zhao H, Xie CG, Guan GJ, Wang DP, et al. J Phys Chem B 2006;110:8613–8.
[58] Gao YX, Yu SH, Guo XH. Langmuir 2006;22:6125–9.
[59] Qi LM, Li J, Ma JM. Adv Mater 2002;14:300–3.
[60] Mann S. Angew Chem Int Ed 2000;39:3392–406.
[61] Yang HR, Su YL, Zhu HJ, Zhu H, Xie BQ, Zhao Y, et al. Polymer 2007;48:4344–51.
[62] Albeck S, Weiner S, Addadi L. Chem Eur J 1996;2:278–84.